Available online at www.sciencedirect.com
SCIENCE DIRECT®
Microporous and Mesoporous Materials 67 (2004) 265–271
MICROPOROUS AND MESOPOROUS MATERIALS
www.elsevier.com/locate/micromeso

Photoionization of methylphenothiazine and photoluminescence of erbium 8-hydroxyquinolinate in transparent mesoporous silica films by spin-coating on silicon

Jae Young Bae [a], Oun-Ho Park [a], Ji-In Jung [a], Koodali T. Ranjit [b], Byeong-Soo Bae [a,*]

[a] *Laboratory of Optical Materials and Coating (LOMC), Department of Materials Science and Engineering, Korea Advanced Institute of Science and Technology (KAIST), 373-1 Kusong-dong, Yusong-gu Daejeon 305-701, South Korea*
[b] *Department of Chemistry, University of Houston, Texas 77204-5003, USA*

Received 5 March 2003; accepted 17 November 2003

Abstract

Transparent mesoporous silica films were successfully prepared by spin-coating on silicon wafers at room temperature. The X-ray diffraction patterns of the films indicate that both hexagonal and cubic mesoporous films can be formed by varying the surfactant to silicon mole ratio. These films have reasonable thermal stability and are calcinable up to 670 °C and crack free when thickness is less than 0.5 μm. The calcined films have a thickness of 433 ± 2 nm as measured by cross-sectional scanning electron microscopy. Methylphenothiazine was incorporated into the mesoporous silica films and after photoionization by ultraviolet light, the radical cation photoproduced was characterized by electron spin resonance spectroscopy. Erbium 8-hydroxyquinolinate was incorporated into the mesoporous silica films and the mesoporous silica films with incorporated Er(III) were characterized by photoluminescence and isothermal nitrogen physisorption studies. The characteristics of the silica films were studied by X-ray diffraction, thermal gravimetric analysis, scanning electron microscopy, high resolution transmission electron microscopy, atomic force microscopy, Fourier transform infrared spectroscopy and isothermal nitrogen physisorption.

Keywords: Photoionization; Electron spin resonance; Photoluminescence; Mesoporous silica films

1. Introduction

Scientists at Mobil Corporation synthesized silica-based mesoporous molecular sieves with hexagonal, cubic, and lamellar structure called M41S materials in 1992 [1]. Zhao et al. [2,3] and Kimura et al. [4,5] reported the successful formation of mesoporous hexagonal aluminophosphate and silicoaluminophosphate by a modified ion-pair process. Recently, hexagonal mesoporous silicoaluminophosphate possessing improved thermal stability (calcinable up to 670 °C) was synthesized by utilizing charge density matching with optimal composition and stirring conditions at room temperature [6,7].

For possible applications of mesoporous oxide materials as sensors and optical materials, it is important to develop thin film materials. Zhao et al. [8] reported dispersion of a bulk silica phase into a liquid which was dip-coated onto silicon wafers and glass slide and resulted in a continuous, uniform coating of colloidal particles. Ogawa [9] described a rapid synthesis route for films in which a mixture of tetramethylorthosilicate is hydrolyzed under acid conditions with substoichiometric amounts of water and cetyltrimethylammonium chloride and then spin-coated on glass substrates. The highest application promise is the use of mesoporous silica films as low dielectric constant (k) materials with k preferable lower than 2.

In the present study, optically transparent and crack-free mesoporous silica films have been synthesized by an evaporation-induced self-assembly process and spin-coated on silicon. These films show thermal stability up to 670 °C. Methylphenothiazine is incorporated into

* Corresponding author. Tel.: +82-42-869-4119; fax: +82-42-869-3310.
E-mail address: bsbae@kaist.ac.kr (B.-S. Bae).

1387-1811/$ - see front matter © 2003 Elsevier Inc. All rights reserved.
doi:10.1016/j.micromeso.2003.11.011

these films and photoionization yields stable radical cations. Methylphenothiazine has excellent electron donating capacity because of its low oxidation potential. This property leads to the formation of charge-transfer complex with numerous electron acceptors. Also, on oxidation it colors and hence can be used to construct electrochromic displays. Erbium 8-hydroxyquinolinate is incorporated into these films and erbium-containing silica films were characterized by photoluminescence and isothermal nitrogen physisorption studies. Photosensitive materials are promising for applications such as sensors, optical devices, optical amplifiers, and electrochromic displays [10].

2. Experimental section

2.1. Sample preparation

The transparent mesoporous silica films were synthesized according to Ogawa and Masukawa [11]. The mesoporous silica films were prepared as follows. Tetramethylorthosilicate (TMOS, Aldrich, 98%) was hydrolyzed under acidic conditions (HCl, J.T. Baker, 36.5–38%), and then methanol (CH_3OH, Merck, 99.8%) was added into the hydrolyzed TMOS at room temperature. Finally, cetyltrimethylammonium chloride (CTACl, Aldrich, 25%) was added so that the final reactant mole ratios were 1–3TMOS:8–16H_2O:0.09–0.11HCl:18–30CH_3OH:0.2–0.8CTACl. The mixture was allowed to react for further 24 h at room temperature to achieve oligomerization. This mixture was concentrated by evaporation of the solvent using a rotary evaporator with vacuum at 40 °C. The solution was dropped onto a spinning (as purchased) silicon wafer substrate (5 cm × 5 cm × 0.6 mm) at a spinning rate of 5000 rpm. Mesoporous thin films were obtained upon complete evaporation of the solvent in a drying oven at 60 °C. The mesoporous thin films were calcined in flowing air at 550 °C for 12 h at rate of 1 °C min^{-1} to remove the organic template.

2.2. Characterization of mesoporous silica films

The transparent silica films were characterized by various methods as follows. X-ray diffraction (XRD) patterns of all mesoporous silica films were obtained on a Rigaku D/MAX-RC diffractometer with CuKα radiation (40 kV, 80 mA) at 0.01° step width and 1 s step time over the range $1.2° < 2\theta < 10°$. Thermogravimetric analysis (TGA) of the silica films was performed on a TGA 2050 analyzer from TA Instruments with a heating rate of 10 °C min^{-1} in oxygen. High resolution transmission electron micrographs (HRTEM) of the calcined silica films were recorded on a JEOL JEM 3010 electron microscope operating at 300 kV. The silica film was detached from the silicon substrate, dispersed in ethanol, and then deposited and dried on a holey carbon film on a Cu grid. Scanning electron microscopy (SEM) images were recorded on a Philips 535M apparatus operating at 20 kV. The surface roughness of the silica films was measured by an atomic force microscopy (AFM) with an Autoprobe 5M from Park Scientific Instruments. Infrared spectroscopy was measured by a Bruker EQUINOX55 FT-IR. N_2 adsorption isotherms were measured at 77 K using a Micromeritics Gemini 2375 analyzer. The volume of adsorbed N_2 was normalized to standard temperature and pressure. Prior to adsorption measurements the calcined samples were dehydrated at 250 °C for 3 h. The BET specific surface area was determined from the linear part of the BET equation ($P/P_0 = 0.05$–0.31). The calculation of the pore size distribution was performed using the desorption branches of the N_2 adsorption isotherms and the Barrett–Joyner–Halenda (BJH) formula [12]. Although the BJH analysis underestimates the pore size [13–16], relative changes in the pore size should be accurately portrayed. The cumulative mesopore (1.7–10.0 nm) surface area, A_{BJH}, was obtained from the pore size distribution curves.

2.3. Incorporation and photoionization of methylphenothiazine and photoluminescence of erbium 8-hydroxyquinolinate

Methylphenothiazine (Aldrich) was incorporated into the silica films by impregnation. The silica films were placed into 10 ml of 1×10^{-2} M methylphenothiazine (Aldrich) in benzene for overnight in the dark. Benzene was removed by flowing nitrogen gas over the sample for 30 min. Erbium 8-hydroxyquinolinate (ErQ, Gelest) was incorporated into the silica films by impregnation. The silica films were placed into 10 ml of 1.5×10^{-3}–1.5×10^{-2} M erbium 8-hydroxyquinolinate in ethanol. Ethanol was removed by flowing nitrogen gas over the sample for 30 min. After drying, erbium 8-hydroxyquinolinate impregnated silica films was dried at 200 °C for 1 h on a hot plate.

The silica films with incorporated methylphenothiazine were irradiated using a 300 W Cermax xenon lamp (ILC-LX 300 UV) at room temperature. The incoming light was passed through a 10 cm water filter to prevent infrared radiation and through a Corning no. 7-54 filter to filter light of wavelengths shorter than 320 nm. The samples were placed in a quartz Dewar and rotated at a speed of 4 rpm to ensure even irradiation. The ESR spectra were recorded at room temperature at 9.5 GHz using Bruker ESP 300 spectrometer and JEOL FE-2XG ESR spectrometer with 100 kHz field modulation and low microwave power to avoid power saturation. Photoproduced methylphenothiazine cation radicals yields were determined by double integration of the ESR

spectra using the ESP 300 software. Erbium 8-hydroxyquinolinate impregnated into the silica films was characterized by photoluminescence (PL) measurements. For infrared PL spectrum of erbium 8-hydroxyquinolinate into the silica films, 477 nm line of Ar ion laser was chosen because it does not coincide with any of the resonant excitation bands of Er^{3+}, thus giving a good feasibility of a broad-band excitation source. The pump power was 200 mW. PL radiation is detected with a monochromator (Digikrom DK240) and a thermoelectrically cooled InGaAs *p-i-n* photo diode (Hamamatsu G5832-23). A general lock-in technique, low noise current preamplifier (Stanford Research SR570) and lock-in amplifier (EG&G 5210) were used for PL signal amplification. With the help of a personal computer, we controlled the PL measurement system and analyzed the PL signals.

3. Results and discussion

3.1. Mesoporous silica films

XRD patterns of as-synthesized and calcined mesoporous silica films in Fig. 1(a) and (b) indicate that a mesoporous structure is formed on the silica substrate. XRD patterns show a prominent peak at $2\theta = 2.0$–$4.0°$ and some broad peaks at $2\theta = 4.0$–$7.0°$ characteristic of hexagonal structure, which is similar to the XRD of hexagonal MCM-41 materials [17]. The unit cell parameter (a_0) [18–21] for a hexagonal structure is calculated from $d(100)$ according to $(a_0) = 2d(100)/3^{1/2}$ where $d(100)$ is obtained from the 2θ value of the first peak in the XRD pattern from $d(100) = \lambda/2\sin\theta$ [22] where $\lambda = 0.15417$ nm for the CuKα line. The unit cell parameter a_0 is equal to the internal pore diameter plus one pore wall thickness. As-synthesized mesoporous silica film shows a $d(100)$ value of 4.3 nm and unit cell parameter of 5.0 nm.

According to the XRD patterns, the mesoporous structure is retained even after decomposition of CTACl by calcination at 550 °C in flowing air for 12 h. The XRD of calcined mesoporous silica film is similar to that prior to calcination except for a substantial decrease in $d(100)$ to 2.6 nm with a unit cell parameter of 3.0 nm. The broadening of the $d(100)$ peak on calcination suggests less structural ordering in the film after calcination.

In addition to preparation of hexagonal mesoporous silica film, materials with cubic phase were also synthesized by varying the surfactant to silicon mole ratio. At a surfactant/Si ratio of less than 0.25, the predominant phase is hexagonal as shown in Fig. 1(a) and (b). As the surfactant/Si ratio increases beyond 0.25, a cubic phase is produced as shown in Fig. 1(c) and (d).

After heating cubic mesoporous silica film in flowing air for 12 h at increasing temperature the XRD patterns are as shown in Fig. 2. XRD patterns of cubic mesoporous silica film show a prominent peak at $2\theta = 2.0$–$4.0°$ and some broad peaks at $2\theta = 4.0$–$7.0°$ characteristic of a cubic structure which are similar to those of cubic MCM-48 materials [17,23]. As-synthesized cubic films show a $d(100)$ spacing of 4.4 nm and a unit cell parameter of 5.1 nm. The cubic structures are retained even after decomposition of CTACl by calcination at 670 °C in flowing air for 12 h. XRD patterns of

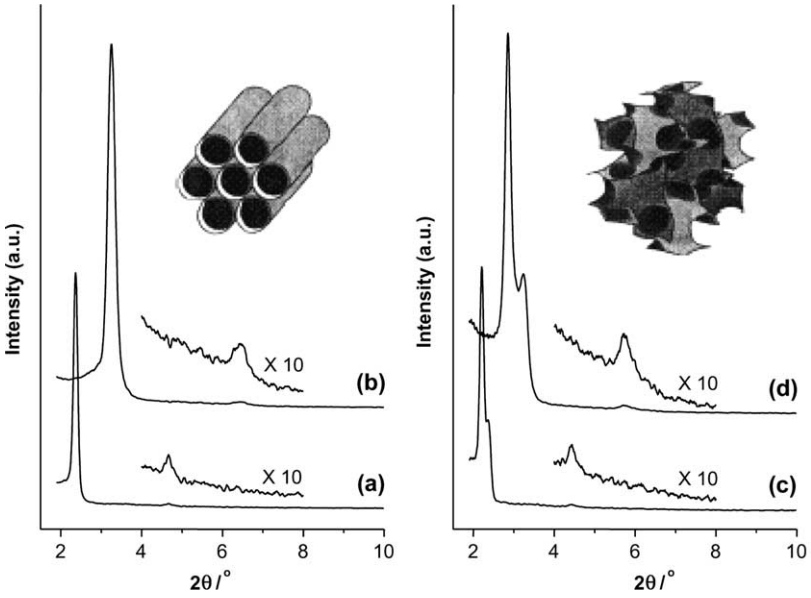

Fig. 1. XRD patterns of (a) as-synthesized, (b) calcined hexagonal mesoporous silica films, (c) as-synthesized and (d) calcined cubic mesoporous silica films.

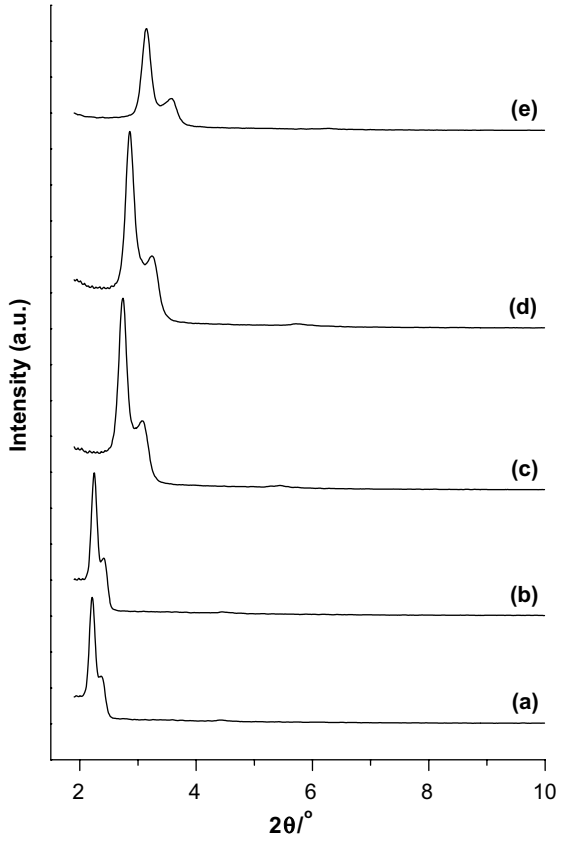

Fig. 2. XRD patterns of cubic mesoporous silica film after being subjected to heat treatment in flowing air for 12 h at increasing temperature (a) as-synthesized, (b) 100 °C, (c) 300 °C, (d) 500 °C and (e) 670 °C.

calcined cubic mesoporous silica films exhibit a broad diffraction peak corresponding to a $d(100)$ spacing of 3.5–2.6 nm and a unit cell parameter of 4.0–3.0 nm. The broadening of the $d(100)$ peak on calcination suggests less order after calcination. The $d(100)$ spacing decreases about 0.9–1.8 nm for calcined versus as-synthesized materials.

Stable mesoporous thin films were reported in 1996 by several groups [9,24,25]. Typically, substrates were introduced into silica/surfactant/solvent systems used to prepare bulk hexagonal mesostructures. Under these conditions, hexagonal silica-surfactant mesostructures are nucleated on the substrate with pores oriented parallel to the substrate surface. Beginning with a homogeneous solution of soluble silica and surfactant prepared in methanol/water solvent, preferential evaporation of methanol concentrates the developing film in water, nonvolatile surfactant and silica species. The progressive increase in surfactant concentration drives self-assembly of silica-surfactant mesostructures [26–28]. Using cetyltrimethylammonium chloride as surfactant, we have demonstrated the formation of hexagonal and cubic mesoporous silica films on silicon by using an evaporation-induced self-assembly process.

The ordered structure of the calcined mesoporous silica film was further confirmed by TEM as in Fig. 3(a), which clearly shows a hexagonal periodicity. The calcined mesoporous silica film thickness is 433 ± 2 nm as measured by cross-sectional SEM (Fig. 3(b)). The surface roughness of the calcined film was studied by AFM, and the average roughness is estimated to be less than 2 nm over a length span of 1000 nm (Fig. 3(c)).

TGA of as-synthesized film shows a weight loss about 35% on heating to 550 °C. Three endothermic losses near 60 °C (3% weight loss), 260 °C (22% weight loss) and 320 °C (10% weight loss) are observed. The weight loss at 60 °C is assigned to water desorption. The weight losses at 260 °C and 320 °C are assigned to desorption

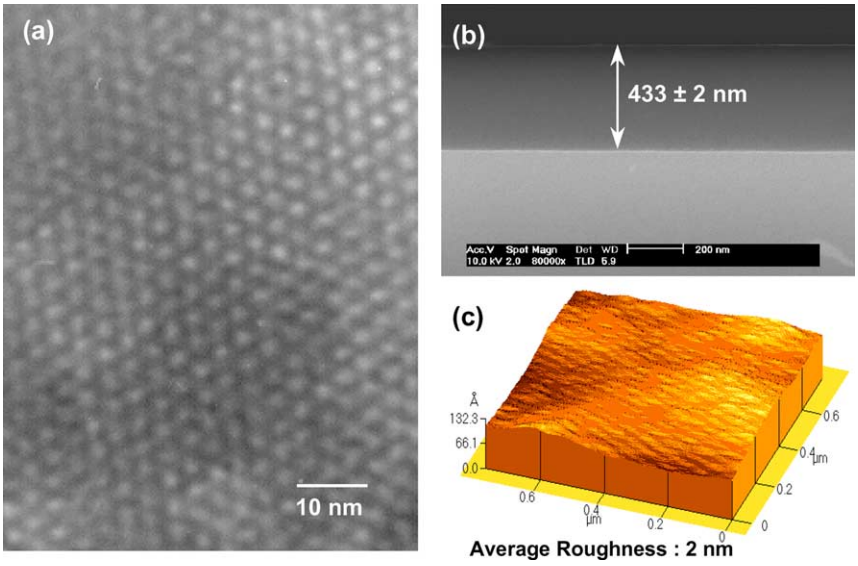

Fig. 3. (a) HRTEM of calcined mesoporous silica films, recorded on a JEOL JEM 3010 electron microscope operating at 300 kV, (b) cross-sectional SEM image and (c) top-view AFM image of calcined mesoporous silica films. The surface roughness of the calcined film is 2 nm.

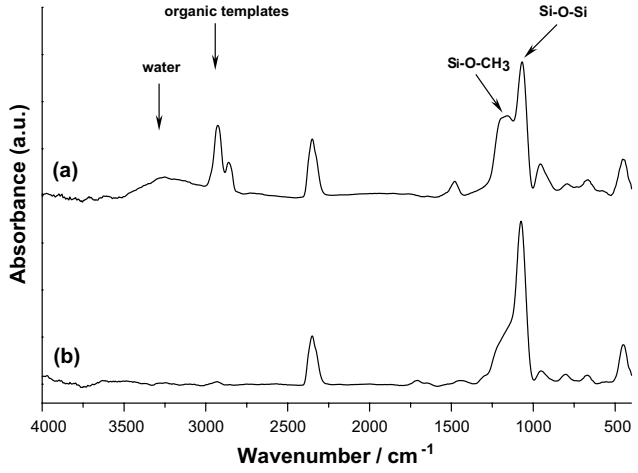

Fig. 4. FTIR spectra of (a) as-synthesized and (b) calcined mesoporous silica films.

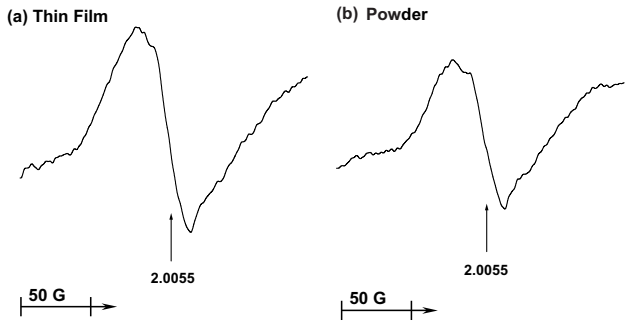

Fig. 5. ESR spectrum of methylphenothiazine cation radical in (a) mesoporous silica film and (b) mesoporous silica powder after being irradiated by 320 nm light at 100 K for 20 min.

and decomposition of CTACl. Nitrogen sorption shows an IUPAC type IV nitrogen adsorption and desorption isotherm. Calcined films have a BET surface area of 920 m^2/g and an average pore diameter of 2.1 nm. The approximate pore size calculation by nitrogen physisorption is smaller than the repeat distance $a_0 = 3.0$ nm determined by XRD because the latter includes the thickness of the pore wall. Thus, we can estimate that the pore wall of these mesoporous silica film is about 0.9 nm thick.

Fig. 4 shows the FT-IR spectra of the as-synthesized and calcined mesoporous silica film. For the as-synthesized film, the band at 2700–3000 cm^{-1} is assigned to the absorption of CTACl and the broad band around 3300 cm^{-1} is assigned to water absorption (Fig. 4(a)). After calcination, the FT-IR spectrum (Fig. 4(b)) shows that CTACl and residual water are efficiently removed. The spectrum shows two additional peaks at 1200 cm^{-1} and 1110 cm^{-1} [29]. The peak at 1100 cm^{-1} is assigned to the absorption of the Si–O–Si bond. The peak at 1200 cm^{-1} is assigned to the absorption of the Si–O–CH_3 bond. After calcination the intensity of the peak at 1100 cm^{-1} increases and the intensity of the peak at 1200 cm^{-1} decreases. This is due to the formation of Si–O–Si bond by the sol–gel process. However, there is an intense shoulder at 1200 cm^{-1} even after calcination indicating the incomplete oligomerization of Si–O–CH_3 to Si–O–Si.

3.2. ESR of mesoporous silica films with incorporated methylphenothiazine

Mesoporous silica films with impregnated methylphenothiazine show a weak ESR signal before ultraviolet irradiation. This indicates that some radicals were produced in the dark prior to irradiation. After irradiation the films turn pink. After being irradiated by 320 nm light at 100 K for 20 min, the samples showed a large ESR signal as shown in Fig. 5(a) [6,7,30]. This ESR spectrum is an asymmetric partially resolved sextet at $g = 2.0055$. The unresolved ESR spectrum of methylphenothiazine in silica films show that the radicals are immobilized at 100 K. The spectral width is the same as that of methylphenothiazine cation radicals in homogeneous solution and in micelles at room temperature, so the spectrum is assigned to such radical [31,32]. The ESR spectrum of methylphenothiazine cation radical exhibits a sextet with the relative intensities of 1:4:7:7:4:1 showing interaction with nitrogen and three protons of methyl group [32–36]. Fig. 5(b) shows the ESR spectrum of impregnated methylphenothiazine in mesoporous silica powder after being irradiated by 320 nm light at 100 K for 20 min. The photoyield of methylphenothiazine cation radical is about 35% higher in the film compared to the powder. The relatively high efficiency of the formation and stablilization of methylphenothiazine cation radical in mesoporous silica films suggest that such films are promising materials for various applications. The lifetime of the methylphenothiazine cation radicals in silica films varies from several hours at 100 K to a few days at room temperature.

3.3. PL of mesoporous silica films with incorporated erbium(III)

Nitrogen adsorption–desorption isotherm of the mesoporous silica film with incorporated Er(III) is shown in Fig. 6(b), confirming its pore accessibility. BET analyses of the sorption isotherms indicate that the mesoporous silica film with incorporated Er(III) reduces the surface area from 920 to 725 $m^2 g^{-1}$ and an average pore diameter from 2.1 to 2.0 nm [37], which suggest that the mesoporous silica film with incorporated Er(III) is completely retained within the pores of the mesoporous silica film as evident from nitrogen sorption isotherm.

Fig. 7 shows the photoluminescence (PL) spectrum of mesoporous silica films with incorporated Er(III). The peak at 1475 nm is due to the gratings in the

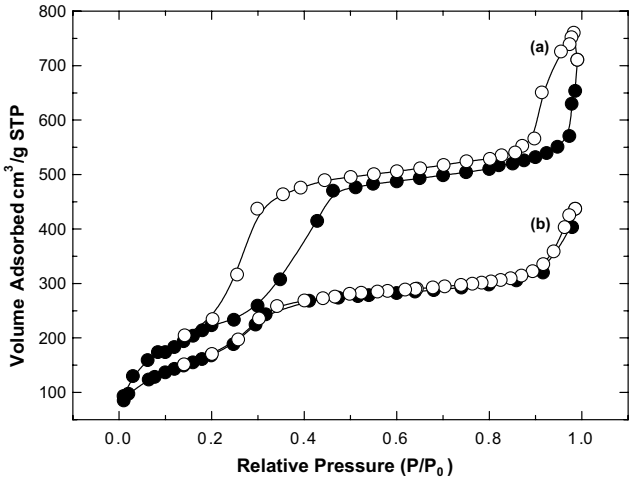

Fig. 6. Nitrogen sorption isotherms for calcined (a) mesoporous silica films and (b) mesoporous silica films with incorporated Er(III).

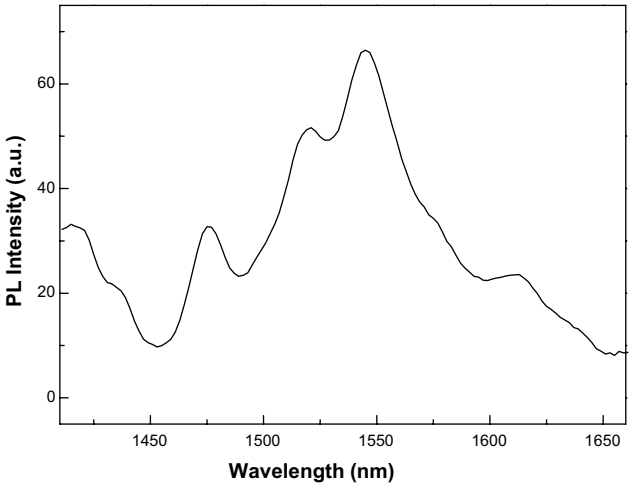

Fig. 7. PL spectra of mesoporous silica films with incorporated Er(III) ($Er/Si = 1.5\times10^{-2}$) at 300 K.

monochromator. The main luminescence peak is at 1545 nm. The bandwidth at half-maximum is 72 nm. The general polymer matrix is not suitable to the incorporation of an Er complex. Theoretically, the most effective method for uniform dispersion is the periodic arrangement of erbium ions in a matrix when high doping levels of Er(III) are required. Thus, we select mesoporous materials as the host matrix. Mesoporous materials have been developed for constructing a periodic pore structure, which has pores of a few nanometers in size. Therefore it is considered that the mesoporous silica film is a good matrix to be doped by a rare-earth complex homogeneously.

The evaporation-induced self-assembly process is a promising method for the preparation of thermally stable and crack free mesoporous silica films.

4. Conclusions

Transparent mesoporous silica films with hexagonal and cubic phases are formed by control the surfactant concentration by an evaporation-induced self-assembly process involving spin-coating on silicon at room temperature. Transparent mesoporous silica films are fairly homogeneous and relatively easy to produce. The mesoporous silica films with hexagonal and cubic phases show possibilities of application as advanced materials. The incorporation of photosensitive materials into mesoporous silica films shows successful photoionization by ESR and PL.

Acknowledgements

This research was supported by grant no. R01-2003-000-10125-0 from the Basic Research Program of the Korea Science and Engineering Foundation and the Brain Korea 21 project.

References

[1] C.T. Kresge, M.E. Leonowicz, W.J. Roth, J.C. Vartuli, J.S. Beck, Nature 359 (1992) 710.
[2] D. Zhao, Z. Luan, L. Kevan, Chem. Commun. (1997) 1009.
[3] D. Zhao, Z. Luan, L. Kevan, J. Phys. Chem. B 101 (1997) 6943.
[4] T. Kimura, Y. Sugahara, K. Kuroda, Chem. Commun. (1998) 559.
[5] T. Kimura, Y. Sugahara, K. Kuroda, Chem. Mater. 11 (1999) 508.
[6] J.Y. Bae, K.T. Ranjit, Z. Luan, R.M. Krishna, L. Kevan, J. Phys. Chem. B 104 (2000) 9661.
[7] J.Y. Bae, L. Kevan, Micropor. Mesopor. Mater. 50 (2001) 1.
[8] D. Zhao, P. Yang, G.D. Stucky, Adv. Mater. 10 (1998) 1380.
[9] M. Ogawa, Chem. Commun. (1996) 1149.
[10] D.A. Doshi, N.K. Huesing, M. Lu, H. Fan, Y. Lu, K. Simmons-Potter, B.G. Potter Jr., A.J. Hurd, J. Brinker, Science 290 (2000) 107.
[11] M. Ogawa, N. Masukawa, Micropor. Mesopor. Mater. 38 (2000) 35.
[12] E.P. Barrett, L.G. Joyner, P.P. Halenda, J. Am. Chem. Soc. 73 (1951) 373.
[13] P.I. Ravikovitch, D. Wei, W.T. Chueh, G.L. Haller, A.V. Neimark, J. Phys. Chem. B 101 (1997) 3671.
[14] M. Kruk, M. Jaroniec, A. Sayari, in: M.J. Treacy, B.K. Marcus, M.E. Bisher, J. Higgins (Eds.), Proceeding of the 12th International Zeolite Conference, Materials Research Society, Warrendale, PA, 1999, p. 761.
[15] W.W. Lukens Jr., P. Schmidt-Winkel, D. Zhao, J. Feng, G.D. Stucky, Langmuir 15 (1999) 5403.
[16] M. Kruk, M. Jaroniec, Langmuir 15 (1999) 5279.
[17] J.S. Beck, J.C. Vartuli, W.J. Roth, M.E. Leonowicz, C.T. Kresge, K.D. Schmitt, C.T.-W. Chu, D.H. Olson, E.W. Sheppard, S.B. McCullen, J.B. Higgins, J.L. Schlenker, J. Am. Chem. Soc. 114 (1992) 10834.
[18] S. Oliver, A. Kuperman, N. Coombs, A. Louth, G.A. Ozin, Nature 378 (1995) 47.
[19] A. Sayari, V.R. Karra, J.S. Reddy, J.L. Moudrakovski, Chem. Commun. (1996) 411.
[20] A. Chenite, Y.L. Page, V.R. Karra, A. Sayari, Chem. Commun. (1996) 413.

[21] A. Sayari, J.L. Moudrakovski, J.S. Reddy, Chem. Mater. 8 (1996) 2080.
[22] B.D. Cullity, Elements of X-ray Diffraction, Addison-Wesley, Boston, 1987, p. 87.
[23] S.V. Nitta, V. Pisupatti, A. Jain, P.C. Wayner Jr., W.N. Gill, J.L. Plawsky, J. Vac. Sci. Technol. B 17 (1999) 205.
[24] H.S. Zhou, D. Kundu, I. Honma, J. Eur. Ceram. Soc. 19 (1999) 1361.
[25] I. Aksay, M. Trau, S. Manne, I. Honma, N. Yao, L. Zhou, P. Fenter, P. Eisenberger, S. Gruner, Science 273 (1996) 892.
[26] H. Yang, A. Kuperman, N. Coombs, S. Mamiche-Afara, G.A. Ozin, Nature 379 (1996) 703.
[27] Y. Lu, R. Ganguli, C. Drewien, M. Anderson, C. Brinker, W. Gong, Y. Guo, H. Soyez, B. Dunn, M. Huang, J. Zink, Nature 389 (1997) 364.
[28] P.J. Bruinsma, A.Y. Kim, J. Liu, S. Baskaran, Chem. Mater. 9 (1997) 2507.
[29] M. Ogawa, J. Am. Chem. Soc. 116 (1994) 7941.
[30] Z. Luan, J.Y. Bae, L. Kevan, Chem. Mater. 12 (2000) 3202.
[31] H.J. Shine, D.R. Thompson, C. Veneziani, J. Heterocycl. Chem. 4 (1967) 517.
[32] M.C. Hovey, J. Am. Chem. Soc. 104 (1982) 4196.
[33] C. Lagercrantz, Acta Chem. Scand. 15 (1961) 1545.
[34] E. Crosignani, P. Franzosini, G. Siragusa, L. Zanotti, Arch. Sci. 24 (1961) 153.
[35] S. Odiot, F. Tonnard, J. Chim. Phys. 61 (1964) 382.
[36] C. Bodea, I. Silberg, Rev. Roum. Chim. 10 (1965) 887.
[37] H. Fan, Y. Lu, A. Stump, S.T. Reed, T. Baer, R. Schunk, V. Perez-Luna, G.P. Lopez, J. Brinker, Nature 405 (2000) 56.